JOURNAL OF Materials CHEMISTRY

Synthesis, stability and electrochemical properties of NiAl and NiV layered double hydroxides

Gianni A. Caravaggio,[a] Christian Detellier*[a] and Zbigniew Wronski*[b]

[a]*University of Ottawa, The Ottawa-Carleton Chemistry Institute, Department of Chemistry, Ottawa, ON, Canada K1N 6N5. E-mail: dete@science.uottawa.ca*
[b]*Canada Centre for Mineral & Energy Technology, MTL, 568 Booth St., Ottawa, ON, Canada K1A OG1. E-mail: zwronski@nrcan.gc.ca*

Received 7th June 2000, Accepted 27th November 2000
First published as an Advance Article on the web 6th February 2001

Layered double hydroxides (LDH) containing NiAl or NiV of varying M(II) : M(III) ratios have been prepared by coprecipitation and characterized by XRD, elemental analysis, and FT-IR. The LDHs electrochemical properties were investigated to determine their potential application as positive electrodes in Ni–Cd and NiMH batteries. Analysis of the electrochemical behavior of the LDHs indicates that the performance is not only dependant on the M(II) : M(III) ratios but also on the degree of structural disorder of the material. The well-crystallized Ni_5Al LDH exchanges up to 1.5 electrons in early cycles but is not stable and collapses on oxidative charging to the oxyhydroxide form. The turbostratic Ni_2Al LDH exchanges more electrons (up to 1.6) and is more stable during charging. However, owing to a lower density in comparison to Ni_5Al, it has a poorer loading capacity. The NiV LDHs exchange a maximum of 1.1 electrons due to the high stability of the higher oxidation states of vanadium, and thus are poor candidates for rechargeable materials.

Introduction

Layered double hydroxides (LDH) are hydrotalcite-like materials. They consist of metal brucite type layers ($Mg(OH)_2$ sheets, where octahedra of Mg^{2+} ions, 6-fold co-ordinated to OH^-, share edges to form two-dimensional infinite sheets). Such sheets are positively charged because of partial substitution of divalent metal ions by trivalent ions. The sheets are stacked on top of each other and are held together by electrostatic and hydrogen bonding. The excess positive charge is neutralised by interlayer anions.[1] The chemical composition of the compounds is generally expressed as $M(II)_{1-x}M(III)_x(OH)_2A^-_xB^{2-}_{x/2}$ where M(II) can be Ni^{2+}, Zn^{2+}, Mg^{2+}, Mn^{2+}, *etc.*, M(III): Al^{3+}, V^{3+}, Co^{3+}, Cr^{3+}, *etc.*; A^-: NO^{3-}, Cl^-, *etc.* and B^{2-}: SO_4^{2-}, CO_3^{2-}, *etc.* LDHs are used as adsorbents,[1] catalysts,[2–5] catalyst precursors,[6,7] anionic exchangers,[8] hosts for intercalation compounds,[9,10] and lately have been tested as a possible replacement for β-$Ni(OH)_2$ used in the positive electrode in Ni–Cd and nickel metal hydride secondary batteries.[11,12] In these batteries, β(II)-$Ni(OH)_2$ is transformed reversibly into β(III)-Ni(OOH) during the charging process. On prolonged or fast charging and/or overcharge, β(III)-Ni(OOH) is transformed irreversibly into γ(III+)-Ni(OOH) where III+ denotes a valence higher than 3, typically 3.6. This causes irreversible damage to the electrode because γ(III+)-Ni(OOH) has a larger interlayer spacing (7.6–8.5 Å)[13] than β(III)-Ni(OOH) (4.84 Å), which causes mechanical deformation. On discharge, γ(III+)-Ni(OOH) becomes α(II)-$Ni(OH)_2$, which is unstable in strong alkali and reverts back to β(II)-$Ni(OH)_2$. This sequence is well known and has been described in the Bode diagram.[14]

If it were possible to cycle between the α and γ phases this would be a large advantage over the conventional β(II)–β(III) cycling because of the following reasons:

(1) Less deformation of the electrode during the charge/discharge process because the α-$Ni(OH)_2$ has very similar interlayer spacing to γ-Ni(OOH), ~7.6–8.5 Å *vs.* 6.9 Å respectively.

(2) An increase of the number of electrons exchanged per atom of nickel because of the nickel in the γ phase having an average oxidation state close to 3.6.

Keeping in mind the statements above, and because NiM(III) LDHs have similarities to α-$Ni(OH)_2$ (*i.e.*, they are both metal hydroxides containing nickel, and have similar layer spacings along the crystallographic *c* axis), these LDHs would be a good choice to test as battery materials. Therefore, in this investigation, we have synthesised LDHs of nickel aluminium and LDHs of nickel vanadium of varying M(II) to M(III) ratios. NiAl was chosen because previous work has shown it to be a promising candidates for the positive electrode in Ni–Cd and NiMH.[12,15–17] NiV LDH was chosen because vanadium is known to have high oxidation states; therefore, it might be possible to access these oxidation states to increase the number of exchanged electrons during the cycling process. These materials were characterised by inductively coupled plasma analysis (ICP), elemental analysis (EA), infrared spectroscopy (IR) and X-ray diffraction (XRD). They have also been tested for stability in 6 M KOH and tested in electrochemical cycling experiments.

Experimental

Synthesis

The preparation of the LDHs was performed under a nitrogen atmosphere. Distilled water was deionised to 18.3 MΩ cm^{-1} in resistivity through a Barnstead B-pure deioniser and then was boiled (refluxed) under nitrogen for at least a day before being used for LDH synthesis. The pH values for the LDH synthesis were measured with a VWR scientific model 2000 pH meter fitted with a VWR low maintenance Triode pH electrode with Ag/AgCl internal reference system, sealed reference and built-in thermistor for automatic temperature compensation. The pH meter was always calibrated with pH 7 and pH 10 buffers prior to any measurements. Reagents used were from commercial sources. Two types of LDH, NiAl and NiV, were synthesized with three different M(II) : M(III) ratios for the NiAl LDH and two different ratios for the NiV LDH which are

 DOI: 10.1039/b004542j

This journal is © The Royal Society of Chemistry 2001

Table 1 Loading of the active material and cycling profile of the electrodes

Material	Loading/g (LDH/β-Ni(OH)$_2$)	Activation charge/ A h	Activation discharge/A h	Regular charge/A h	Regular discharge/A h	Slow discharge/A h
Ni_2Al	0.6234	0.009	0.018	0.045	0.180	0.036
Ni_2Al	0.6469	0.009	0.019	0.047	0.187	0.037
Ni_5Al	0.8609	0.018	0.024	0.059	0.236	0.047
Ni_5Al	0.7747	0.012	0.025	0.062	0.249	0.050
Ni_9Al	0.9185	0.013	0.027	0.066	0.265	0.053
Ni_9Al	0.9100	0.013	0.026	0.066	0.263	0.053
Ni_2V	0.7134	0.010	0.021	0.052	0.206	0.041
Ni_2V	0.6933	0.010	0.020	0.050	0.200	0.040
Ni_5V	0.8394	0.012	0.024	0.062	0.243	0.049
Ni_5V	0.8400	0.012	0.024	0.061	0.243	0.049
β-Ni(OH)$_2$	1.2354	0.018	0.036	0.089	0.357	0.071
β-Ni(OH)$_2$	1.2200	0.018	0.035	0.088	0.353	0.071

shown below:

$$NiAl = 2:1, 5:1, 9:1$$

$$NiV = 2:1, 5:1$$

The synthesis of NiV LDH with a 9 : 1 ratio was attempted but only Ni(OH)$_2$ was obtained.

Ni_2AL and Ni_5Al LDHs were synthesized using the method of Wang *et al.*[18] A mixture consisting of $Ni(NO_3)_2{\cdot}6H_2O$ (58.16 g, 0.20 mol, Aldrich 99.1%) and of $Al(NO_3)_3{\cdot}9H_2O$ (37.51 g, 0.10 mol, Aldrich 98+%) in 300 ml of freshly boiled deionised water was added together with a 2 M NaOH (BDH 98%) solution (~200 ml) to a flask containing 150 ml of deionised water. Rapid stirring was maintained throughout the addition and the rate of addition was such that the pH was kept at 10±0.5. After the addition was completed, the mixture was heated at ~75–80 °C for 16 h under N_2. It was then filtered, washed with water then dried at 70 °C for 24 h. Ni_5Al was prepared in the same fashion but the nickel and aluminium nitrates were weighed to obtain the appropriate molecular ratios.

The Ni_9Al LDH was prepared using the method of Kamath *et al.*[11] It was impossible to obtain such a low aluminium ratio using the Wang *et al.*[18] method. A mixed metal nitrate solution (210 mL) of $Ni(NO_3)_2{\cdot}6H_2O$ (21.99 g, 0.076 mol, Aldrich 99.1%) and of $Al(NO_3)_3{\cdot}9H_2O$ (3.15 g, 0.0084 mol, Aldrich 98+%) was added dropwise (~3 mL min^{-1}) to 210 mL solution of NaOH (8.4 g, 0.21 mol, BDH 98.0%) containing sodium carbonate (3.00 g, 0.28 mol, Aldrich 99.5+%) at 35 °C. The mixture was heated at 65 °C for ~16 h and was filtered with large amounts of water until a neutral pH was obtained. The sample was dried at 65 °C. All the samples were ground in a mortar and pestle until a fine powder was obtained.

Ni_2V and Ni_5V LDHs were obtained using a modified version of the Rives method.[19] Preparation was performed under a nitrogen atmosphere. A 200 mL solution containing $NiCl_2{\cdot}6H_2O$ (47.54 g, 0.20 mol, Aldrich 97.2%) and VCl_3 (15.79 g, 0.10 mol, Aldrich 98.1%) was added dropwise to 250 mL of a Na_2CO_3 (21.19 g, 0.20 mol, Aldrich 99.5+%) and NaOH (28 g, 0.7 mol, BDH 98.0%) solution at room temperature. The solution was stirred for ~2 h then the volume was reduced to *ca.* 50%. It was filtered hot and washed with water until no Cl^- was detected. The samples were dried in air.

Characterization

XRD patterns were obtained using a Philips PW3710 diffractometer with Cu-Kα radiation ($\lambda = 1.54059$ Å, 2θ: 8° to 72°). Elemental analyses of the metals were carried out on a Jarrell Ash Atom Scan model inductively coupled plasma emission spectrometer (ICPES) after dissolution in a 2 : 5 v/v mixture of nitric and hydrochloric acid. C, H, and N elemental analysis was carried out with a Perkin Elmer Series II CHNS/O 2400 elemental analyser (EA). Infrared spectra were recorded using a Bomem MB-100 model Fourier transform infrared spectrometer (FT-IR). Specimens were tested in the form of KBr pellets. The densities of the materials were determined with a Micromeritics multivolume model 1305 pycnometer.

Stability testing

To determine the stability of NiAl and NiV LDH in the caustic conditions found in alkaline batteries, the LDHs were immersed in 6 M KOH at room temperature and were analyzed by XRD and IR over a period of time up to a maximum of one and a half months. For these tests, 0.5 g of material was immersed in 50 mL of 6 M KOH. The samples were removed at predetermined intervals, rinsed with water until neutral pH, dried, and a portion of them was analyzed by XRD and IR. The materials were then reimmersed into a freshly prepared solution of 6 M KOH after the analysis.

Electrode testing

Pasted electrodes were prepared from NiAl, NiV LDHs and β-Ni(OH)$_2$ (commercial battery grade) powders. For each electrode the LDH or Ni(OH)$_2$ powder was mixed with Ni extra-fine filamentary powder, (Inco, type 210), Co powder, water and polyvinyl alcohol, and then mixed to create a paste. A porous nickel foam (INCOFOAM 98% porosity) substrate, cut to dimensions of 4 × 12 cm and 8 mm thick, was manually filled with the paste and dried at 100 °C for 1 h. This sheet was rolled into a 0.75 mm thick strip from which three circular electrodes were punched. The typical loadings of the LDH powders or β-Ni(OH)$_2$ in the porous structure of the pasted electrodes are shown in Table 1. Two of the electrodes were cycled in flooded half-cell conditions in a 6/1 molar KOH/LiOH electrolyte. The cycling was performed using an Arbin model multichannel potentiostat/galvanostat (battery cycler) at room temperature (22.5±2.5 °C). Potentials of the cells were measured against the (INCOFOAM) nickel metal foam.

Table 1 gives the cycling conditions used for testing the NiAl, NiV LDHs and the reference β-Ni(OH)$_2$ powders. All the electrodes were soaked for 24 h in the KOH before the activation charge and discharge steps. These steps consist of charging the material for 35.6 h at a rate that is 20 times less than the regular charge, and discharged for 8.1 h at a rate that is 10 times less than a regular discharge. The electrodes were then charged (regular charge) at the rates shown in Table 1 for 4.0 h followed by a regular discharge for 45 min. There was always a one-minute rest period between a charge and a discharge cycle. In addition, every ten cycles the electrodes were discharged at a slow rate (slow discharge = 1/5 of the regular discharge). We adopted this profile because it was an optimized cycling profile for the commercial nickel hydroxide. However, the optimal cycling profile for testing LDHs may require different charging or discharging rates

Table 2 X-Ray powder diffraction data for NiAl LDHs

M(II)/M(III) material	X = Al/Al+Ni	*hkl*	*d* spacing (observed)/Å	Lattice parameters/Å	*d* spacing (Takovite)/Å
Ni_2Al	0.33	003	8.49	$a=3.03$, $c=25.94$	
		006	4.24		
		101	NO[a]		
		012	2.61		
		015	2.24		
		018	1.95		
		110	1.51		
		113	NO[a]		
Ni_5Al	0.16	003	8.04	$a=3.08$, $c=24.03$	7.54
		006	4.00		3.77
		101	2.66		2.61
		012	2.61		2.55
		015	2.32		2.27
		018	2.00		1.92
		110	1.53		1.51
		113	1.51		1.48
Ni_9Al	0.11	003	7.81	$a=3.102$, $c=23.31$	
		006	3.99		
		101	NO[a]		
		012	2.68		
		015	2.33		
		018	1.83		
		110	1.55		
		113	1.50		

[a]Not observable.

Results and discussion

XRD data

The observed *d* spacings (Table 2) of Ni_2Al and Ni_5Al are similar to those quoted in the literature.[2] In addition, the *c* parameter increases with increasing aluminium content, which is also a trend observed for hydroxynitrate LDHs.[2]

The X-ray pattern obtained for the Ni_5Al LDH is characteristic of takovite, which is a hydrotalcite type material (takovite JCPDS 15-87). The reflections could be indexed with a rhombohedral cell. The lattice parameter *c* was determined with the 003 reflection and the *a* parameter was indexed with the d_{001} reflection ($a=2d_{110}$). Each of these parameters is included in Table 2. Note that there is a decrease in the *a* parameter as the aluminium content increases. This is because the Al^{3+} radius is smaller than that of Ni and this agrees with Vergard's law.[1] In addition, the reflections of Ni_2Al and Ni_9Al LDHs are broader and more asymmetrical than those of Ni_5Al LDH (Fig. 1). This is an indication that the stacking sequences of the two former LDHs are more disordered. Some authors refer to these type of materials as being turbostratic.[11,20]

The XRD reflections of both NiV LDHs are broad and asymmetrical indicating the disordered nature of these materials (Fig. 2). These compounds were not hydrothermally treated for long periods of time hence their low crystallinity. The *a* and *c* parameters can be found in the last column of Table 3. The values were calculated in the same way as for the NiAl LDHs. In spite of the fact that the LDHs have different vanadium contents, there is no observed difference for the *a* parameter. This is because the 110 peak is very broad for both samples and an exact value for it was difficult to determine. In contrast to the NiAl LDHs, the *d* spacing decreases as the vanadium content increases. This behaviour is expected because there is higher carbonate content in the Ni_2V LDH due to the higher concentration of V^{3+} in the layers. The higher carbonate content increases the electrostatic interaction between layers hence decreasing the spacing in between them.

IR Analysis

Fig. 3 shows the infrared spectra of Ni_2Al, Ni_5Al and Ni_9Al. Each of these spectra are characteristic of hydrotalcite compounds.[1] The LDHs have the following bands: A broad peak centered at about 3500 cm^{-1} corresponds to the vibration bands of hydroxyl groups hydrogen bonded to water molecules. The H_2O bending vibration can be observed at 1630 cm^{-1}. The sharp and strong band at 1380 cm^{-1} shows clearly the presence of the nitrate ion in each sample. The shoulder at around 1360 cm^{-1} indicates the presence of carbonate ions (v_3 CO_3^{2-}).

As shown by the elemental analyses and the sharp and strong band at 1380 cm^{-1} in the IR spectrum, the predominant anion in the interlayer of the Ni_2Al LDH is the nitrate species. Despite the fact that the nitrate anion is the major interlayer species, there are still carbonate vibrations that are present in the infrared spectra. The very weak but sharp bands at 2420–2440 cm^{-1} and 1750–1760 cm^{-1} represents the v_1+v_3 and v_1+v_4 modes of the carbonate anion. The small band at 692 cm^{-1} is the v_4 of the CO_3^{2-} anion.[7] In the range between 1200–200 cm^{-1} many structural lattice vibrations can be found. The sharp but small bands at 430 cm^{-1}, 562 cm^{-1} are translational modes of oxygen in AlO_6 octahedra and the band at 614 cm^{-1} is assigned to OH groups. According to Espinose de la Caillerie *et al.*[21] the sharpness of these bands is consistent with an ordered distribution of aluminium ions within the octahedral sheets. Finally, the sharp and small band at 825 cm^{-1} can be assigned to the v_2 mode of the nitrate ion.

For the Ni_5Al LDH, even if the carbonate concentration is small, one can observe the bands characteristic of this anion, the v_1+v_3 and v_1+v_4 modes at 2462 and 1760 cm^{-1}. The

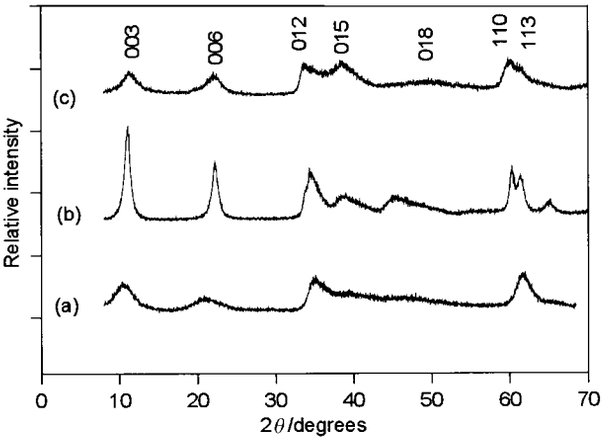

Fig. 1 Powder XRD patterns of (a) Ni_2Al, (b) Ni_5Al and (c) Ni_9Al.

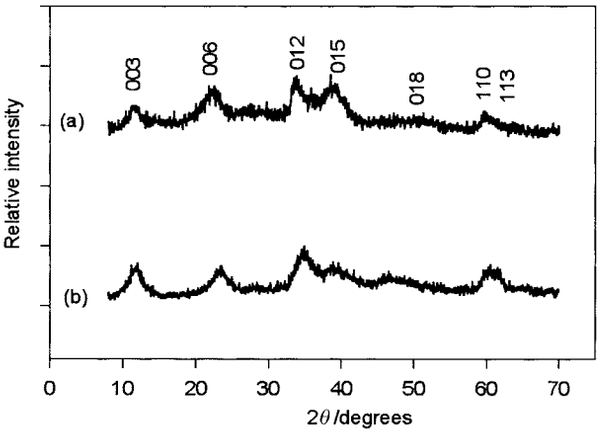

Fig. 2 Powder XRD patterns of (a) Ni_2V and (b) Ni_5V.

Table 3 X-Ray powder diffraction data for NiV LDHs

M(II)/M(III) atomic ratio	X = V/V + Ni	*hkl*	*d* spacing (observed)/Å	Lattice parameters/Å
Ni_2V	0.31	003	7.58	$a = 3.10$, $c = 25.94$
		006	3.801	
		101	NO[a]	
		012	2.57	
		015	2.35	
		018	1.96	
		110	1.55	
		113	1.50	
Ni_5V	0.16	003	7.76	$a = 3.10$, $c = 24.03$
		006	4.01	
		101	NO[a]	
		012	2.65	
		015	2.32	
		018	NO[a]	
		110	1.55	
		113	NO[a]	

[a]Not observable.

Table 4 Elemental analysis and ICPES data

M(II)/M(III) material	Element	Calc. wt%	Exp. wt%	Molecular formula
Ni_2Al	Ni	32.3	34.10	$Ni_{0.67}Al_{0.33}(OH)_2$-$(NO_3)_{0.20}(CO_3)_{0.066}\cdot 0.7H_2O$
	Al	8.09	7.87	
	H	3.09	3.10	
	N	2.51	2.60	
	C	0.72	0.75	
Ni_5Al	Ni	44.8	44.6	$Ni_{0.84}Al_{0.16}(OH)_2$-$(NO_3)_{0.16}\cdot 0.6H_2O$
	Al	3.89	3.90	
	H	2.93	2.88	
	N	2.02	2.03	
Ni_9Al	Ni	51.4	45.7	$Ni_{0.90}Al_{0.10}(OH)_2$-$(NO_3)_{0.02}(CO_3)_{0.042}\cdot 0.4H_2O$
	Al	2.71	2.40	
	H	2.76	2.74	
	C	0.49	1.01	
	N	0.25	0.51	
Ni_2V	Ni	32.9	28.7	$Ni_{0.69}V_{0.31}(OH)_2$-$(CO_3)_{0.155}\cdot 2(H_2O)$
	V	12.8	11.2	
	H	3.77	3.75	
	C	1.51	0.74	
Ni_5V	Ni	46.6	39.0	$Ni_{0.84}V_{0.16}(OH)_2$-$(CO_3)_{0.082}\cdot 0.5H_2O$
	V	8.35	6.62	
	H	2.87	2.91	
	C	0.93	1.64	

shoulder at $\sim 1360\ cm^{-1}$ indicates the presence of the carbonate ion which is in a lower symmetry (C_{2v}) resulting in the activation of the ν_1 band seen at $1078\ cm^{-1}$, inactive when the carbonate anion retains its full symmetry (D_{3h}).[12] Again, below $1200\ cm^{-1}$ the AlO_6 translational modes at $569\ cm^{-1}$, $430\ cm^{-1}$ and at $646\ cm^{-1}$ the ν(OH–OH_2) mode can be observed. The sharp band at $3641\ cm^{-1}$ is characteristic of a non-hydrogen bound OH group normally found in β-$Ni(OH)_2$. This indicates a β-$Ni(OH)_2$ contamination in the sample. However, since the deviation between the experimental chemical analysis and calculated values is low (<2%) one can suppose that the contamination is quite small (Table 4).

In the case of the Ni_9Al LDH the characteristic nitrate bands in C_{2v} symmetry are demonstrated by the shoulder at $1480\ cm^{-1}$ and the band at $1001\ cm^{-1}$. This LDH also shows the carbonate ν_1 vibration mode at $1046\ cm^{-1}$.[22] The lattice bands are at 641, 560 and $430\ cm^{-1}$. The band at $3648\ cm^{-1}$ can also be noted in this sample. It is larger than the one seen in Ni_5Al LDH indicating a larger amount of β-$Ni(OH)_2$ contamination which probably explains the discrepancy between the experimental and the chemical analysis (Table 4).

The infrared spectra of the NiV LDH (Fig. 4) are similar to those of the NiAl LDHs. However, the former were prepared from the metal chloride salts and precipitated in a bicarbonate solution. Therefore, only the carbonated anion can be found in the NiV LDHs since chloride was washed out of the precipitate during filtration. The elemental and IR analyses both confirm this (Table 4). The ν_3 carbonate band at $1357\ cm^{-1}$, without any shoulder, indicates the presence of only this anion in the interlayer sheet. In addition, the band is split due to the lowering of the symmetry of the carbonate and in turn, this lowering of symmetry activates the ν_1 mode of the anion seen at $1077\ cm^{-1}$. Furthermore, centred at about $3450\ cm^{-1}$ we have the OH stretching band of hydrogen bonded hydroxyl groups and water molecules. In contrast to the OH band seen in the IR spectra of the NiAl LDHs, this band is wider due to a weak shoulder around $3200\ cm^{-1}$ indicating the water molecules are hydrogen bonded to carbonates in the interlayer.[23] In the Ni_5V IR spectrum we can see the sharp band at $3635\ cm^{-1}$ due to non-bonded OH groups indicating the presence of β-$Ni(OH)_2$.

Fig. 5(a,b,c) shows the X-ray diffraction patterns obtained at different time intervals in KOH of the three different compositions of the NiAl LDHs (Ni_2Al, Ni_5Al and Ni_9Al).

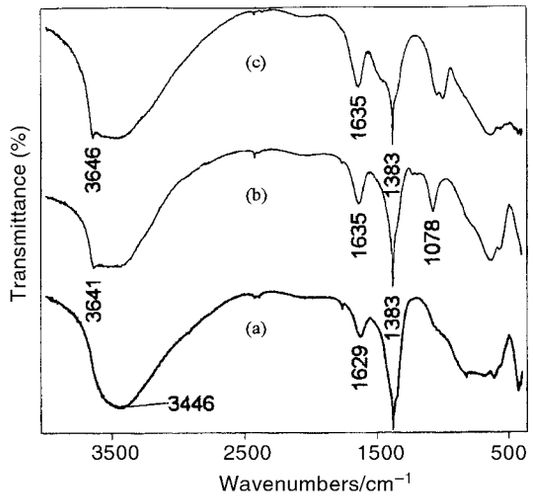

Fig. 3 Infrared spectra of (a) Ni_2Al, (b) Ni_5Al and (c) Ni_9Al.

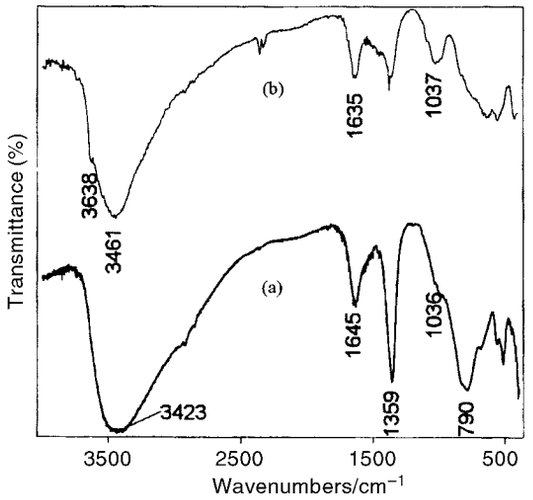

Fig. 4 Infrared spectra of: (a) Ni_2V and (b) Ni_5V.

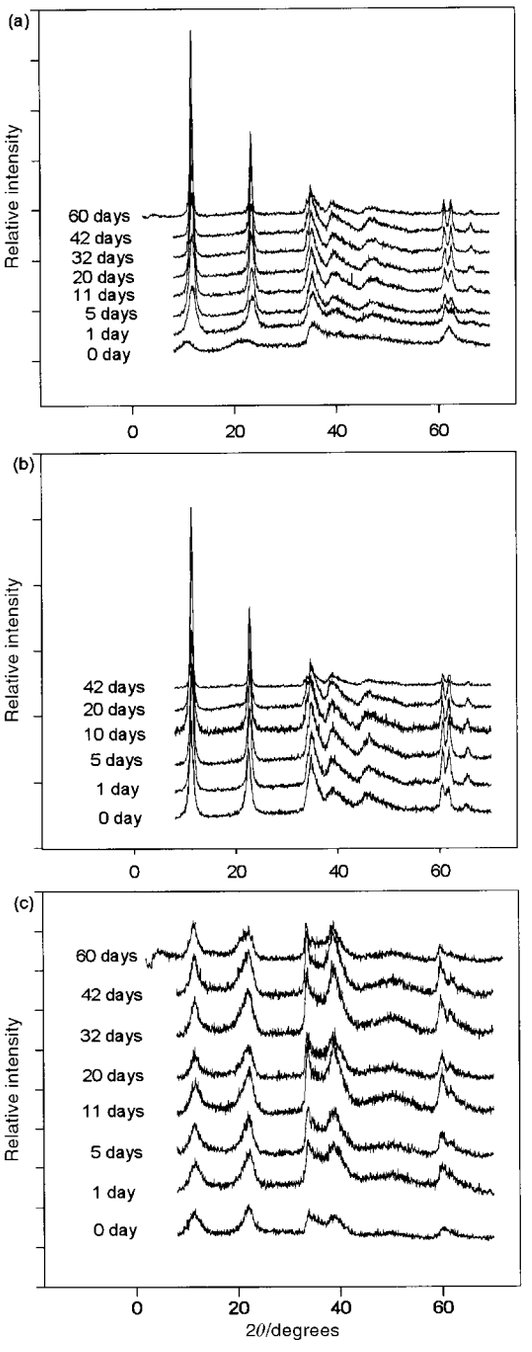

Fig. 5 Powder XRD patterns of the NiAl LDHs aged in 6 M KOH: (a) Ni_2Al, (b) Ni_5Al and (c) Ni_9Al.

The broad lines of the XRD of Ni_2Al at day 0 show the sample begins with a very low crystallinity and as time in the KOH increases the lines of the diffractograms become sharper. This indicates an increase in crystallinity of the sample and confirms the results obtained by Ehlsissen *et al.*[15] where they reported that the LDHs become crystalline as they are aged in KOH. The increase in crystallinity can be explained as a mechanism involving dissolution and a recrystallization process. In addition, the d_{003} spacing is decreased from 8.48 Å to 7.55 Å which is due to the carbonate anion in the interlayer. This anion has stronger electrostatic interaction than the nitrate ion with the metal layers and hence reduces the interlayer spacing. The sample also shows no sign of degradation in KOH as time goes on up to the end of the test. Fig. 5b shows the stability test of Ni_5Al; one can notice an increase in crystallinity of the LDH but this effect is not as pronounced as in the case of Ni_2Al LDH since the starting material is already more crystalline. Furthermore, with ageing, the interlayer spacing does not decrease as much as that of Ni_2Al LDH indicating that there is very little replacement of the interlayer nitrates by carbonates. Because Ni_5Al LDH has less aluminium than Ni_2Al LDH, the former has less of an excess positive charge. Therefore, the carbonate anions would be less attracted inside the layers and this could possibly explain the slow replacement of the nitrate anions. For the duration of the stability test there is also no apparent degradation of this compound as judged by the X-ray diffraction pattern. Finally, Fig. 5c shows the stability test of the Ni_9Al LDH. Contrary to the literature there is seemingly no degradation of this compound even up to two months in the strong alkali (6 M KOH). In addition, the peaks do not get sharper over time in the KOH indicating that there is no increase in crystallinity of the sample. It is stated that an aluminium content where $x > 0.14$ is needed to stabilize the LDH in the alkali medium. Otherwise, if the content is lower than this value, the LDHs are transformed into β-$Ni(OH)_2$ which is apparent by the appearance of a reflection at 4.6 Å after ageing. However, Ehlsissen *et al.*[15] carried out the stability tests in 8 M KOH at 40 °C and in the article by Kamath *et al.*[3] the tests were done in 8 M KOH at room temperature (22 °C to 28 °C). In this study, the LDHs were immersed in 6 M KOH at room temperature, which is in line with the operation of practical sealed cells.

The diffractograms of the stability test of Ni_2V are shown in Fig. 6a. Contrary to the NiAl LDH, Ni_2V is unstable on prolonged ageing in aqueous KOH above 14 days. However, similarly to the NiAl LDHs, the vanadium containing LDHs also become more crystalline when immersed in aqueous KOH, up to 14 days. This can be seen by the sharpening of the d_{003} and d_{006} reflections in addition to the appearance of the d_{101} reflection that could not be seen before the ageing process (Fig. 6a). Unfortunately, between 14 and 34 days there is the appearance of another phase. We note the disappearance of the d_{006} reflection and the appearance of new ones at ~4.3 Å (2θ: 20.7°) and 2.7 Å (2θ: 33.2°). Finally, after 40 days the transformation is in its advanced stages. The new phase was found to be β-$Ni(OH)_2$. This was determined by comparing the diffractogram obtained after 40 days of ageing with a diffractogram of β-$Ni(OH)_2$. It can be concluded that the Ni_2V LDH is only stable up to 14 days in 6 M KOH after which it starts to transform into β-$Ni(OH)_2$.

The diffractograms of Ni_5V LDH are found in Fig. 6b. For this LDH, we can observe the appearance of the β-$Ni(OH)_2$ phase after only 5 days and the transformation is complete between 20 and 42 days. Since Ni_5V has less V^{3+} in the layers than Ni_2V there is less electrostatic interaction holding the layers together. Therefore, it was expected that Ni_5V LDH would be less stable than Ni_2V in aqueous KOH.

From the results obtained from the stability tests, it is clear that the NiAl LDHs are more stable than the NiV LDHs. This is most likely because Al^{3+} (0.044) has a larger charge over radius than V^{3+} (0.038) allowing stronger electrostatic interaction in the layers.

Cycling performance

Fig. 7a and 8a show the number of exchanged electrons (NEE) per atom of nickel as a function of cycle number for the NiAl and the NiV LDHs and that of a commercial β-$Ni(OH)_2$ powder. The NEE for each powder was calculated using the formula below

$$\mathrm{NEE} = 3600 C_{\mathrm{exp}}/nF$$

where C_{exp} is the experimental discharge capacity in A h g^{-1} of LDH in the electrode, n is the number of moles of nickel per gram of LDH, and F is Faraday's constant (96485 C mol s^{-1}).

According to Fig. 7a, the electrodes containing Ni_2Al and

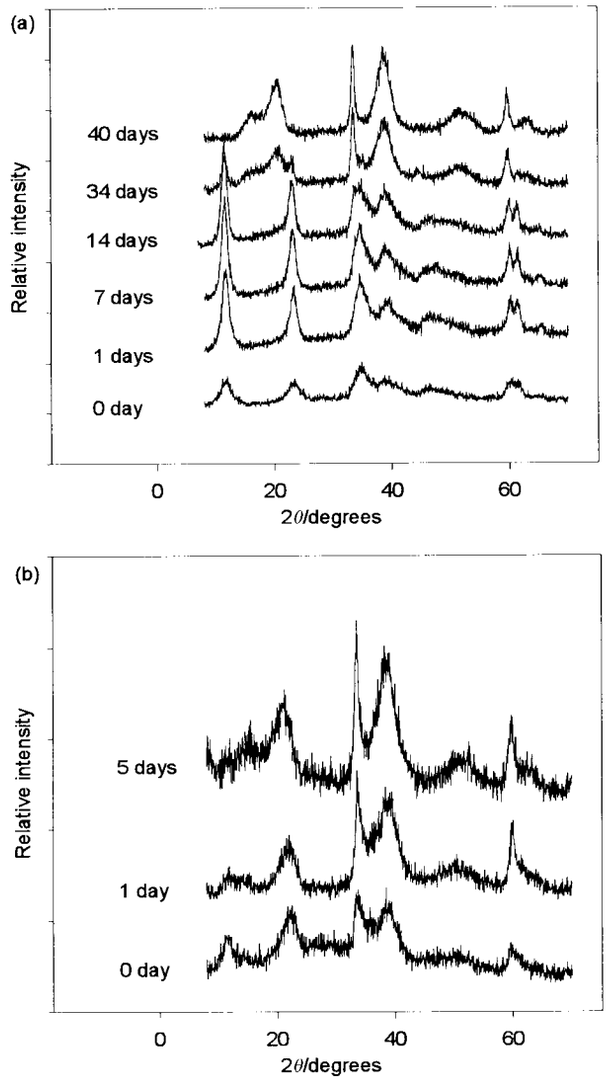

Fig. 6 Powder XRD patterns of the NiV LDHs aged in 6 M KOH: (a) Ni_2V and (b) Ni_5V.

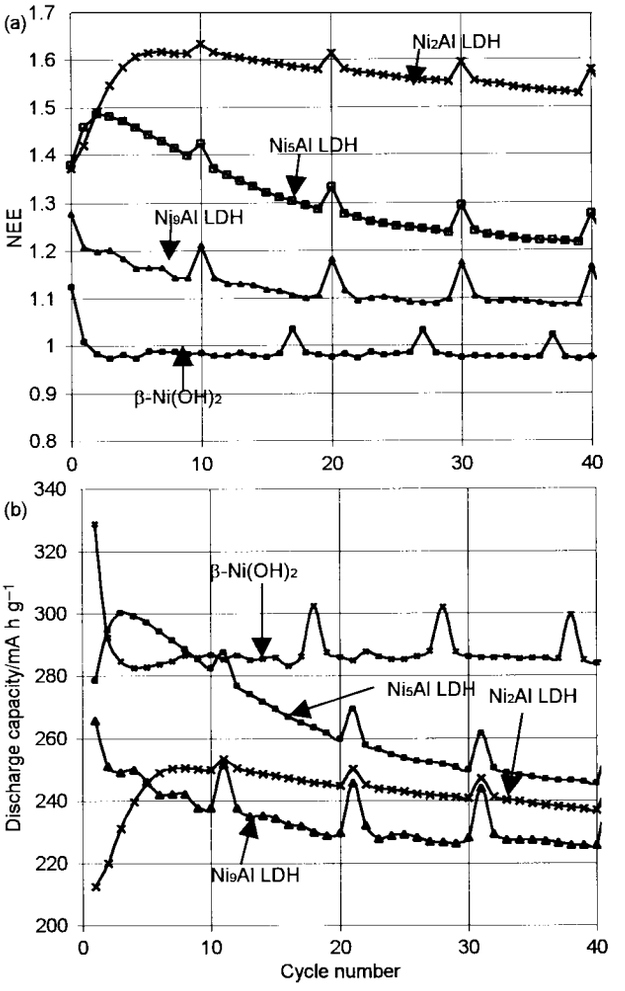

Fig. 7 (a) Number of exchanged electrons (NEE) and (b) gravimetric discharge capacity as a function of cycles for the NiAl LDHs and the commercial nickel hydroxide powders.

Ni_5Al LDH obtain their maximum discharge/charge capacity within 5 to 10 cycles. The NEE of Ni_2Al is higher than that of Ni_5Al, and Ni_5Al has a higher NEE than Ni_9Al. All three LDHs have higher NEE than the commercial $Ni(OH)_2$. It is known that on discharging from γ-$Ni(OH)_2$ to α-$Ni(OH)_2$ it is possible to exchange up to 1.6 electrons. This is because the nickel atoms in γ-$Ni(OH)_2$ have an average oxidation state of 3.6 due to some nickel atoms found in a $+4$ oxidation state.[24] Since the LDHs stabilize the α-nickel hydroxide phase, cycling between the α-$Ni(OH)_2$ and the γ-$Ni(OH)_2$ can occur and more electrons can be exchanged.

Preliminary long-term experiments, up to 500 cycles, have also been performed on these materials. In these tests, the NEE of all the LDHs decreases as the cycle number increases. A possible explanation is that the material is transforming into β-$Ni(OH)_2$, and then cycles between the β(II) and β(III) phases, thus resulting in the decrease in the NEE. Even though the stability tests showed that the materials were stable in the harsh alkali conditions, the stability tests did not take into account the harshness of charging and discharging the material. Another possibility for the decrease in the NEE may be in the fabrication of the electrodes. If the electrodes are overloaded with the LDH powder, the material does not bind properly to the nickel foam. During the cycling it may detach itself from the nickel foam support and lose contact with the metallic electron conductor, effectively reducing the active material on the electrode and lowering the NEE. Finally, the combination of both processes might also be possible.

Fig. 8a shows the number of exchanged electrons (NEE) per atom of nickel as a function of cycle number for the two NiV LDHs and that of a commercial $Ni(OH)_2$ powder. These materials also level their discharge capacity at about 5 to 10 cycles. The trend of NEE is similar to that of NiAl LDHs. That is, Ni_2V containing the largest amount of vanadium has the highest NEE. Both NiV LDHs have higher NEE than the commercial β-$Ni(OH)_2$. Preliminary long-term experiments have also been done with these materials. The NEE of Ni_5V decreased quicker than that of Ni_5Al. The former reached the NEE of the commercial powder at about 90 cycles which corresponded to approximately the same time as the complete transformation to β-$Ni(OH)_2$ as determined by the stability test (about 20 days). Ni_2V reached the NEE of the beta nickel hydroxide at about 400 cycles ($\sim$80 days). This would then most likely correspond to the complete transformation of the LDH into β-$Ni(OH)_2$.

Fig. 7b shows the NiAl LDH and $Ni(OH)_2$ gravimetric discharge capacity as a function of cycle up to 40 cycles. The gravimetric capacity is given as the number of mA h per gram of LDH or per gram of nickel hydroxide for the commercial powder. The Ni_5Al begins with the highest capacity but after 15 cycles goes below the commercial nickel hydroxide. It however keeps the highest capacity of all the LDHs in this cycling range. Ni_2Al LDH has the second highest capacity followed by Ni_9Al LDH. In spite of the fact that Ni_2Al has the highest NEE it does not have the highest gravimetric capacity. To understand

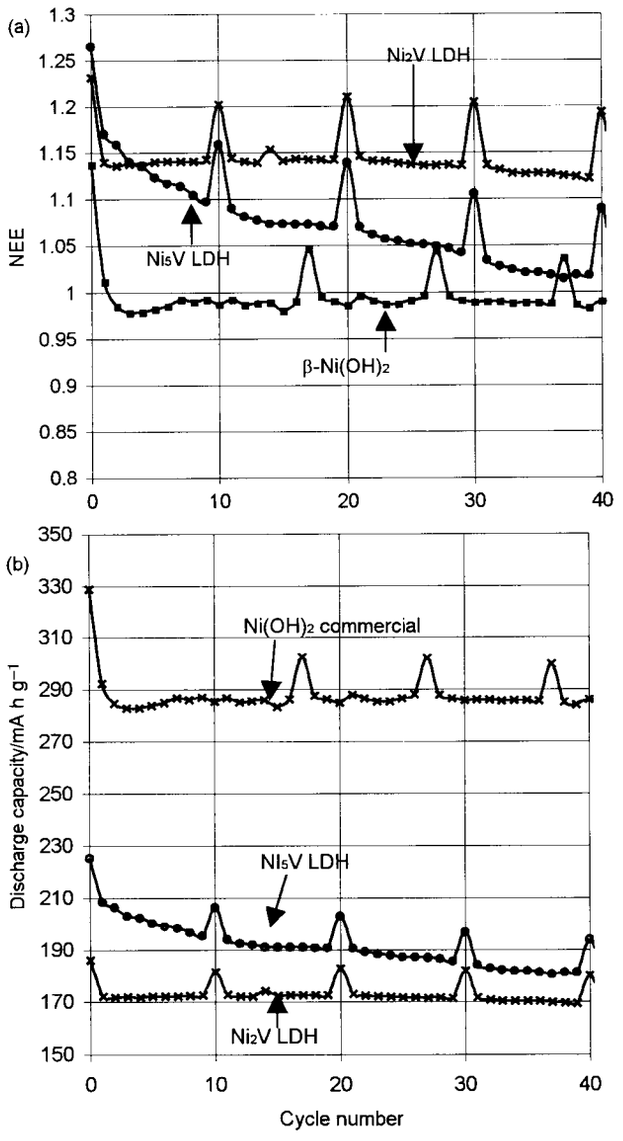

Fig. 8 (a) Number of exchanged electrons (NEE) and (b) gravimetric discharge capacity as a function of cycles for the NiV LDHs and the commercial nickel hydroxide powders.

these results one must not only take into account the number of exchanged electrons but also look at the quantity of LDH that was pasted inside the electrode. There is 28% more Ni_5Al LDH pasted in the electrode than Ni_2Al. Therefore, when the capacity values of the electrodes containing Ni_2Al are corrected for the weight difference and for the difference in the number of exchanged electrons, we are able to obtain gravimetric capacities similar to those electrodes containing Ni_5Al LDH ($<2\%$ deviation). As for the electrodes containing Ni_9Al LDH, on average 42% more material of LDH was pasted inside the electrode. However, when the capacities of the electrodes containing Ni_2Al were corrected for this weight difference and corrected for the difference in the number of exchanged electrons, the corrected values were larger than the experimental values by about $\sim$5–8%. On the long term, Ni_2Al appears to keep the highest capacity of all the LDHs, which is in agreement with the fact that it is the most stable LDH.

Fig. 8b shows the gravimetric discharge capacity of the NiV LDHs. The gravimetric capacity of the Ni_5V LDH is higher than that of the Ni_2V LDH in this range of cycle numbers. The Ni_5V containing electrodes contain $\sim$19% more material than the Ni_2V containing electrodes. When the gravimetric capacities of the Ni_2V containing electrodes are corrected for the difference in mass and for the NEE, these correction factors are

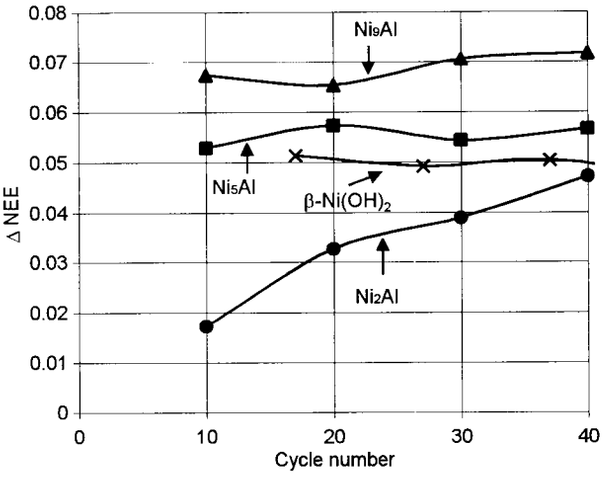

Fig. 9 The difference between the NEE of the slow and fast discharges of the NiAl LDHs.

valid up to about 15 cycles after which the deviation between the corrected capacity and the experimental one is larger than 5%. The reason for the difference in the quantity of powder pasted in the electrode is most certainly due to the difference in bulk densities of the materials. Ni_2Al with the smallest density (2.60 g mL^{-1}) has less powder pasted in the electrode followed by Ni_5Al (2.97 g mL^{-1}) and finally Ni_9Al (3.00 g mL^{-1}). The same can be said for the NiV LDHs since Ni_2V has a density of 2.38 g mL^{-1} and Ni_5V and Ni_2V have bulk densities of 2.66 g mL^{-1} and 2.38 g mL^{-1}. Knowing this, an increase of the bulk density of the powders by milling them and making them finer, allowing the powder to pack more densely, would be a good way to maximize the LDH properties as battery materials. It has already been demonstrated by Wronski[25] that β-$Ni(OH)_2$ powders when milled for several hours in a vibratory ball mill exhibit an improvement in the discharge capacity by 10% to 20% and outstanding stability up to at least 800 cycles.

In Fig. 7 and 8 the spikes are the result of the cells being discharged at a slower rate during these cycles than the rest of the cycles. During a slow discharge, more electrons are being extracted from the material than during a regular discharge. This is because during the regular discharge, the formation of a layer of a relatively non-conductive hydroxide phase near the surface of the particles can force a large fraction of the discharge current to travel through alternative electrical paths, instead of reducing the oxyhydroxide material. The slow discharge promotes a more homogeneous supply of electrons, a better access to the core of the unreduced oxyhydroxide particulates, thus giving a better utilisation of the active mass and consequently higher discharge capacity of the electrode material. As determined in the Bode[14] diagram during a discharge there is a gain of protons for the exchange of every electron in the β(II)/β(III) or the γ(III+)/α(II) cycle. Therefore, during a slow discharge there is a larger quantity of electrons and protons being exchanged than during a regular discharge for the same period.

Fig. 9 shows the difference between the slow and fast discharge of the cells containing the different powders. These data give us some insight into the kinetic aspects of the cycling. The difference in the NEE between the slow and fast discharge increases from Ni_2Al, Ni_5Al, and Ni_9Al LDH. A small difference between the slow and fast discharge indicates that not only the electrons but also the protons, which must accompany the redox electron exchange on cycling, become more available in the Ni_2Al structure. Consequently, the reduction of the more conductive active mass becomes less dependent on the discharge rate. This graph therefore indicates that the Ni_2Al LDH has greater proton availability than Ni_5Al

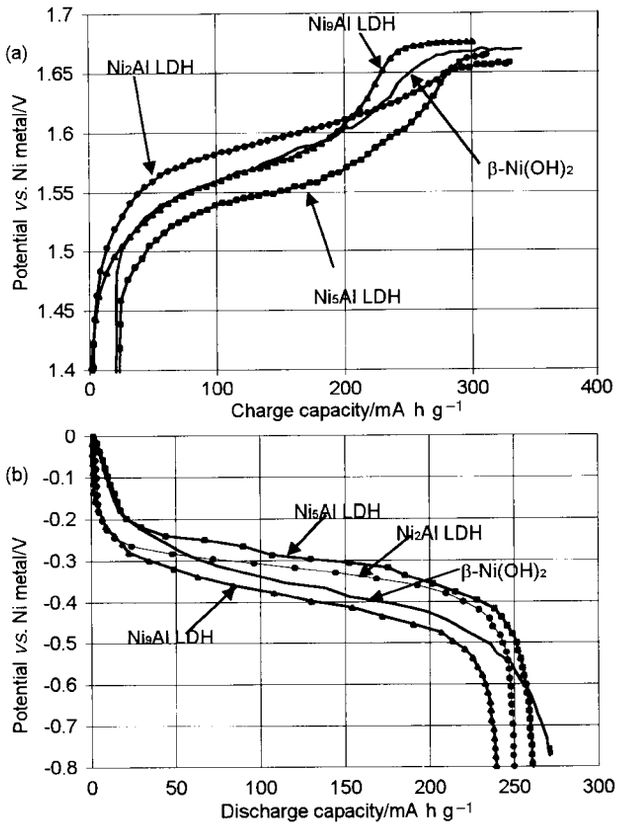

Fig. 10 (a) Charge and (b) discharge curves for the β-$Ni(OH)_2$ and the NiAl LDHs at cycle number 9.

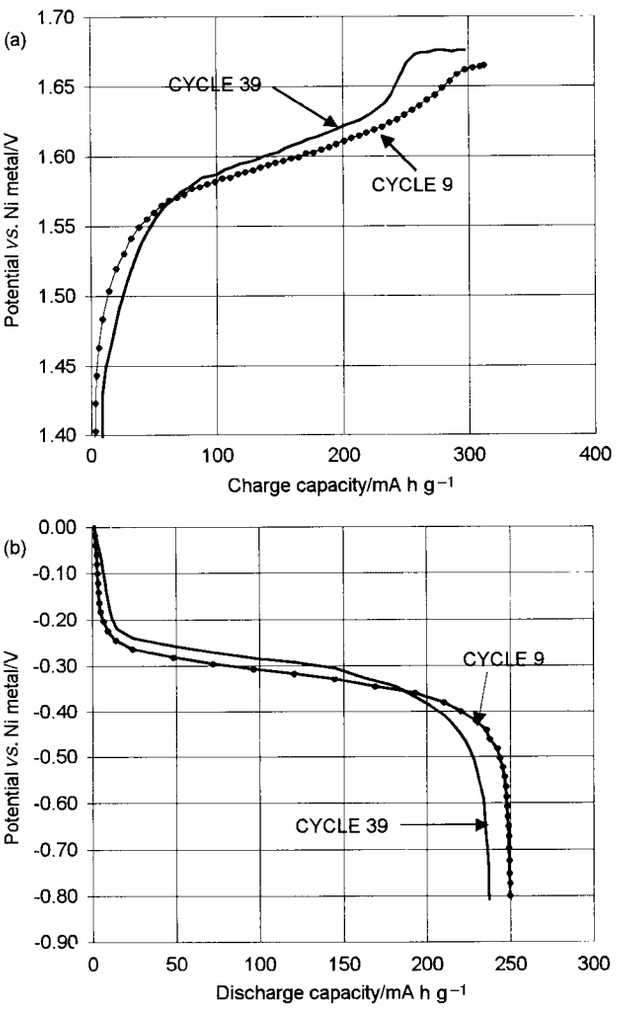

Fig. 11 (a) Charge and (b) discharge curves for the Ni_5Al LDH at cycle numbers 9 and 39.

and Ni_9Al LDHs, and that this availability decreases as the cycle number increases. The increase in availability may be a result of an increase in Brønstead acidity of the hydroxyl groups attached to the aluminium atoms. This may control the onset of proton exchange between neighbouring OH groups. The decrease in availability of protons as shown by the increase in the difference between the fast and slow discharge as cycle number increases could be an indication of the LDHs becoming β-$Ni(OH)_2$.

Potential curves collected during charging and discharging are shown in Fig. 10–13. The curves collected during charging at cycle 9, Fig. 10a, show that the plateau corresponding to the oxidation of the hydroxide is shorter for the crystalline Ni_5Al LDH than for the β form, and the potential of oxidation of active mass is lower by about 25 mV. This behavior emphasizes good charging characteristics and easy insertion of protons in the well-spaced planes of LDHs. The oxidation of the LDH proceeds as a single reaction until the charge capacity reaches approximately 200 mA h g^{-1}. Afterwards, further oxidation of the LDH strongly competes with some other process, which is reflected in the gradual potential increase until the oxygen evolution potential is reached. One can observe a change in the slope for this increase. Only the last and distinct part of the gradual increase can clearly be related to oxygen evolution, which results from the electrolyte decomposition. This gives rise to the possibility that the slope may be related to a gradual collapse of the plates as the charging proceeds. Indeed, comparing cycles 9 and 39 (Fig. 11a) one can conclude that the oxygen evolution is well separated from the oxidation of the LDHs' active mass at higher cycles, because the gradual slope disappears, however the oxygen evolution potential remains the same.

Fig. 10a shows that the charging plateau for the turbostratic Ni_2Al LDH is much longer than either the plateau of the Ni_5Al LDH or the β-nickel hydroxide. The potential value for this plateau is approximately 50 mV higher than that of the Ni_5Al LDH and 25 mV higher than that of β-nickel hydroxide. However, the oxygen evolution potential is slightly lowered in comparison to both the well-crystallized Ni_5Al LDH and the β form. Since the charging curve at cycle 9, Fig 12a, is not very distinct from the curve at cycle 39, the turbostratic structure results in a better stability for the Ni_2Al LDH on cycling than the crystalline structure of the Ni_5Al counterpart.

The charging plateau for Ni_9Al LDH occurs at potential values similar to the β form, although the plateau is much shorter due to the oxygen evolution which starts earlier in the charging process. From cycles 9 to 39 (Fig. 13), there is little change in either the charging or the discharging curves.

The differences in the charging profiles are reflected in the discharge curves Figs. 10b, 11b and 12b, respectively. For the well-crystallized Ni_5Al LDH the plateau voltage is substantially higher (almost 100 mV) than for the β hydroxide, and the low aluminium content Ni_9Al LDH (Figs. 10b, 13b). Although the curves for cycles 9 and 39 follow each other during the first part of the discharge process the plateau at cycle 39 is much shorter in the crystalline form of the LDH (Ni_5Al) than in the turbostratic form (Ni_2Al). Therefore, the discharge capacity fades on cycling to a lesser degree in a turbostratic form, *i.e.*, a poorly crystallized LDH.

The charge and discharge behavior of turbostratic Ni_2V shows little change from cycles 9 to 39. Its discharge plateau at cycle 9 is more flat, yet shorter, than that for the almost amorphous Ni_5V. The number of exchanged electrons in both NiV LDHs (*ca.* 1.1) is only slightly higher than in the β-nickel hydroxide (NEE = 1). This means V does not contribute to the

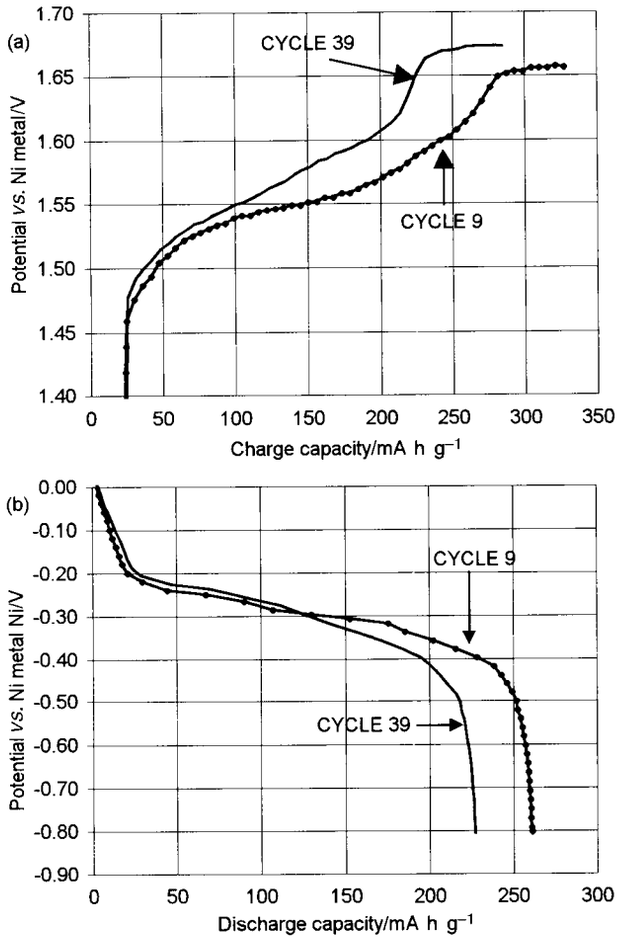

Fig. 12 (a) Charge and (b) discharge curves for the Ni_2Al LDH at cycle numbers 9 and 39.

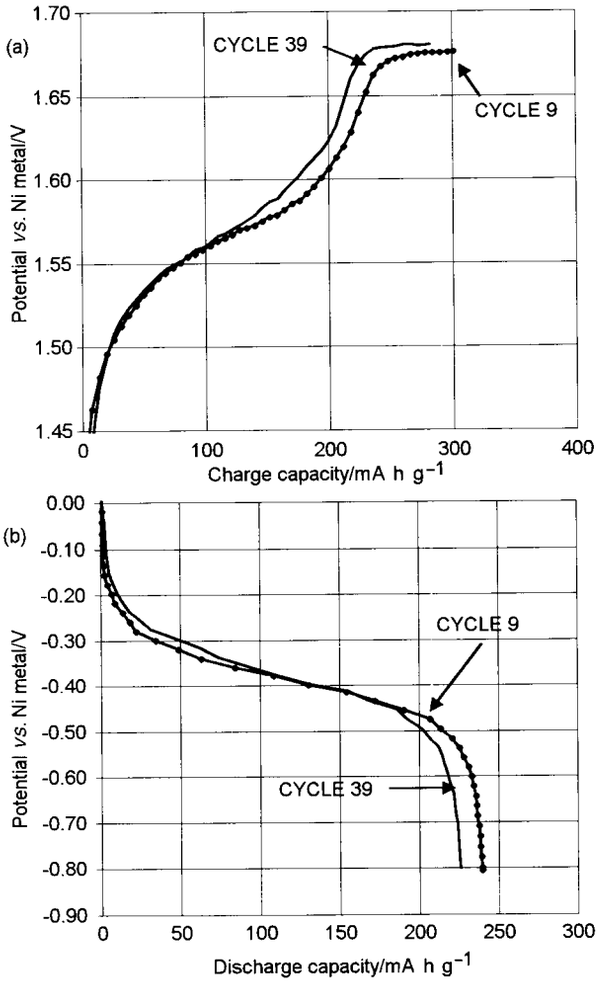

Fig. 13 (a) Charge and (b) discharge curves for the Ni_9Al LDH at cycle numbers 9 and 39.

reversible electrochemical redox process. As much as this is disappointing the finding can be explained by the high stability of the higher oxidation state of vanadium. The discharge capacity is poor due to the low density of the powder which is not compensated by the higher electron exchange observed in NiAl LDHs. Therefore NiV LDHs seem to be poor candidates for active mass in Ni rechargeable batteries.

Conclusions

(1) As the amount of aliovalent metal increases the LDH structure changes from disordered to crystalline to turbostratic to amorphous (V). Yet, the electrochemical performance of LDHs does not depend on a concentration of an aliovalent metal (Al or V) only, and is dependent on the degree and the kind (*e.g.* turbostratic, amorphous) of structural disorder.

(2) The well-crystallized Ni_5Al LDH exchanges up to 1.5 electrons in early cycles, exhibits long and flat plateaux, but is not stable and collapses on oxidative charging to the oxyhydroxide form, which is accompanied by oxygen evolution.

(3) The turbostratic NiAl LDH exchanges as many or more electrons and is more stable during oxidative charging.

(4) The discharge plateau becomes longer but more sloping when going from a crystalline LDH to a disordered, to a turbostratic, and finally to an amorphous LDH.

(5) The NiV LDHs exchange only up to 1.1 electrons in early cycles as would be expected from the high stability of the higher oxidation state of vanadium. Thus, it is a poor candidate for a rechargeable battery material.

(6) The turbostratic Ni_2Al LDHs, *viz.* Ni_5Al, would be good candidates for active mass in the Ni positive electrode, if only a spherical high-density morphology powder form could be developed, which would improve loading of these powders in electrodes. This would merit further investigation of "poorly crystallized" *viz.* turbostratic LDHs.

Acknowledgements

The Natural Science and Engineering Research Council of Canada and the Ontario Graduate Scholarships in Science and Technology are gratefully acknowledged for research grants. The authors would like to acknowledge Daniel Martineau for technical help for the electrode cycling experiments and Arvin Moser for fruitful discussions.

References

1 F. Cavani, F. Trifiro and A. Vaccari, *Catal. Today*, 1991, **11**, 173.
2 E. C. Kruissink and L. L. Van Reijei, *J. Chem. Soc., Faraday Trans. 1*, 1981, **77**, 649.
3 A. L. Mackenzie, C. T. Fishel and R. J. Davis, *J. Catal.*, 1992, **138**, 547.
4 T. Nakatsura, H. Kwasaki, S. Yamashita and S. Kohjiya, *Bull. Chem. Soc. Jpn.*, 1979, **52**(8), 2449.
5 R. S. Mulukutla and C. Detellier, *J. Mater. Sci. Lett.*, 1997, **16**(9), 752.
6 S. Gusi, F. Pizzoli, F. Trifiro, A. Vaccari and G. Del Piero, *Prep. Catal.*, 1987, 753.
7 C. Busetto, G. Del piero, G. Manara, F. Trifiro and A. Vacari, *J. Catal.*, 1984, **85**, 260.
8 D. L. Bish, *Bull. Mineral.*, 1980, **39**, 170.

9 L. Raki, D. G. Rancourt and C. Detellier, *Chem. Mater.*, 1995, **7**, 221.
10 N. Herbert, A. Clearfield and E. F. Vansant, *Microporous Mesoporous Mater.*, 1998, **23**, 97.
11 P. V. Kamath, M. Dixit, L. Indira, A. K. Shukla, V. G. Kumar and N. Munichandraiah, *J. Electrochem. Soc.*, 1994, **141**(11), 2956.
12 A. Sugimoto, S. Ishida and K. Hanawa, *J. Electrochem. Soc.*, 1999, **146**(4), 1251.
13 D. Singh, *J. Electrochem. Soc.*, 1998, **145**, 116.
14 H. Bode, K. Dehmelt and J. Witte, *Electrochim. Acta*, 1966, **11**, 1079.
15 K. T. Ehlsissen, A. Delahaye-Vidal, P. Genin, M. Figlarz and P. Willmann, *J. Mater. Chem.*, 1993, **3**(8), 883.
16 L. Indira, M. Dixiy and V. Kamath, *J. Power Sources*, 1994, **52**, 93.
17 B. Liu, X. Y. Wang, H. T. Yuan, Y. S. Zhang, D. Y. Song and Z. X. Zhou, *J. Appl. Electrochem.*, 1999, **29**, 855.
18 J. D. Wang, Y. Tian, R. C. Wang and A. Clearfield, *Chem. Mater.*, 1992, 1276.
19 V. Rives and F. M. Labajos, *Inorg. Chem.*, 1993, **32**, 5000.
20 Z. S. Wronski, G. J. C. Carpenter, D. Martineau and P. J. Kalal, *Electrochem. Soc. Proc.*, 1997, **97-18**, 804.
21 J. Espinose de la Caillerie, M. Kermarec and O. Clause, *J. Am. Chem. Soc.*, 1995, **117**, 11471.
22 M. J. Hernandez-Morena, M. A. Ulibarri, J. L. Rendon and C. J. Serna, *Phys. Chem. Miner.*, 1985, **12**, 34.
23 F. M. Labajos, M. D. Sastre, R. Trujillano and V. Rives, *J. Mater. Chem.*, 1999, **9**, 1039.
24 W. E. Grady, K. I. Pandya, K. E. Swider and D. A. Corrigan, *J. Electrochem. Soc.*, 1996, **143**(5), 1616.
25 Z. S. Wronski, Extended abstract, *Symp. Electrochem. Power sources after 200 years*, ISE Meeting, Parvia, Italy, Sept. 1999..